

NUMERICAL INVESTIGATIONS OF A SPENT FUEL STORAGE POOL IN ABNORMAL CONDITIONS

J-p Simoneau¹, B. Gaudron¹, Jérôme Laviéville², Julien Dumazet¹

Electricité de France (EDF)

¹12-14, av. Dutriévoz, 69628 Villeurbanne cedex, France

²6, quai Watier - 78401 Chatou cedex, France

jan-patrice.simoneau@edf.fr; bruno.gaudron@edf.fr; jerome-marcel.lavieville@edf.fr

ABSTRACT

This paper deals with the thermal behavior of spent fuel storage pools, in the situations of loss and restart of the forced cooling system. The objective is to set up methodologies for the modeling of the two phase flow behavior. A first approach is performed with a single phase code (*Code_Saturne*). A simplified boiling model is then implemented considering flashing below the free surface. An agreement with in situ measurements is obtained for the natural convection flow occurring in normal conditions and in the first hours after the loss of cooling. In a second step a more detailed multiphase modeling is set up, thanks to the *Neptune_CFD* code. The boiling inside the pool and the heat and mass transfers at the free surface are simultaneously calculated. The early times computed are analyzed and compared positively with the single phase simplified model. Finally, further steps are described.

KEYWORDS

Spent fuel pool, CFD, Boiling, Two-phase flow

1. INTRODUCTION

The thermal behavior of spent fuel storage pools is of first importance to ensure the safety of nuclear installations. In this respect, one important safety criterion for spent fuel assemblies' integrity is to maintain a liquid water level over the assemblies. Some previous analyses can be found in [1] and [2]. In nominal conditions, a forced water cooling circuit ensures low temperatures inside the pool and hence an efficient fuel heat removal at constant water level. In abnormal conditions (loss of cooling circuit), boiling may occur locally or globally in the pool to remove spent fuel thermal power. Safety water injection maintains liquid water at normal operating level but the restart of the cooling pumps can be subject to cavitation or steam suction when the saturation margin is low.

The objective of this paper is to better understand the thermal behavior of the pool in that accidental situation thanks to CFD analyses applied on a generic case. The scenario will first be described in section 2, highlighting some specific characteristics of this kind of flow. The first approach, based on a single phase calculation with the CFD software *Code_Saturne* [3], is described in section 3, where boiling is modeled in a simple way as regards to the saturation temperature. In section 4, the multiphase software *Neptune_CFD* [4] allows a more precise description of the boiling phenomenon. However, its combination with the water / air free surface representation leads to some difficulties and the calculations presented are a first step.

A general analysis and perspectives are then provided in section 5.

2. DESCRIPTION OF THE CONSIDERED SCENARIO

2.1. Pool Operating

The spent fuel storage pool of PWRs consists in a quasi rectangular parallelepiped volume with the order of magnitude of the characteristic length being 10 m. This domain is filled with a height of about 15 m of water, the spent fuel assemblies (about 4 m length) being located in its bottom part. A dedicated circuit removes the decay heat power by injecting cold water and extracting hot water. Forced convection occurs during this normal operation and several inlets and outlets ensure an almost homogeneous low temperature.

The fuel assemblies are set vertically inside racks, in the bottom of the pool. Those racks are open cells so that water can enter and circulate easily.

2.2. Incidental Transient

In case of loss of the forced cooling circuit, the decay heat is no more removed via this device and a natural convection loop develops inside the pool. Decay heat first increases the water temperature since the losses are now limited to heat transfer to the concrete walls and to the surrounding air via the free surface. After a delay, saturation temperature may be reached and heat starts to be removed by evaporation and mass transfer to the atmosphere.

Due to the hydrostatic pressure, the saturation temperature increases with the depth so that boiling is more likely to occur close to the free surface. However, under saturated nucleate boiling may also happen in the fuel assemblies, depending on the competition between natural cooling flow and surface heat flux density. Later during the transient, make-up water is injected inside the pool in order to compensate the evaporated water. The regulation is set to maintain liquid water level as for normal operations.

When the event ends with the cooling circuit recovery, the pumps restart may be affected by cavitation or steam suction because water temperature and pressure may be close to the saturation at cooling system intake. Due to pressure losses, dynamic pressure and turbulence, the instant static pressure can reach values below the boiling point.

2.3. Method

The numerical approach is based on a stepwise approach, considering an increasing complexity and the validation state of the different CFD codes.

Prior to all, a physical analysis is performed, since it drives the modeling. Figure 1 presents a scheme of a spent fuel pool and the different physical phenomena involved and the expected two phase occurrence.

Considering that, with the positive effect of hydrostatic pressure, boiling is willing to appear only in the upper part of the pool near the free surface, one can consider that steam flow may have a low influence on liquid flow. The first step of the method is then the use of a single phase approach. A steady state calculation is run to obtain an equilibrium state by considering that decay heat is only removed via boiling and subsequent mass transfer, by keeping liquid water at saturation temperature (depending on pressure).

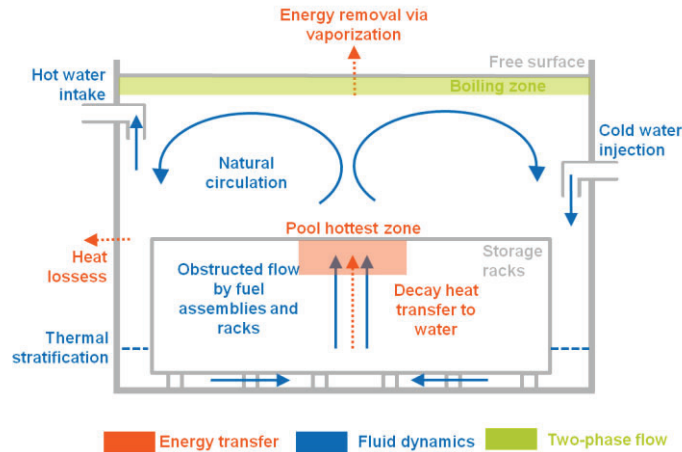


Figure 1 Spent fuel pool physical phenomena

In that way, boiling is taken into account with the energy balance without effect on mass and momentum balance. Such a model would be acceptable under two conditions:

- The water level variation (including the water refill) is low beside the total height of the pool.
- The boiling zone remains localized near the free surface, and does not modify significantly the velocity field in the pool. The bubbles are removed directly and do not condensate elsewhere in the pool.

A transient computation is then applied to assess the saturation margin at the intake region in case of restart of the forced cooling circuit.

The second step employs a multifield CFD code, and models both the boiling phenomenon and the water / air free surface behavior. Physically speaking, this approach is much more comprehensive because the effect of multiphase flow is taken into account for energy, mass and momentum balances. It mainly involves the use of two different sets of models for interfacial exchanges (for boiling and free-surface) which are generally made to run separately, and which can hence represent a potential difficulty.

The initial objective was to model first the level variation due to water removal and the following refilling process. The cooling circuit restart with two-phase models is not yet considered here, nor the cavitation analysis which will be done further thanks to the instant pressure field and literature correlations.

3. SINGLE PHASE BASED APPROACH

3.1. Modeling

3.1.1. Domain and grid

The domain considered is representative of a generic spent fuel pool and not linked to a specific reactor design (see Figure 2). The back wall appears in cyan, the spent fuel racks, including vertically positioned assemblies, are in red and the pink parts represent the intake and exhaust pipes of the forced cooling circuit, the labeled ones are those considered for the present calculation of pumps restart.

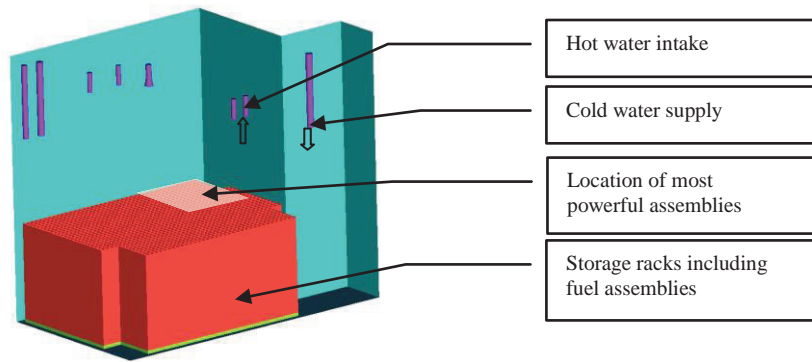


Figure 2 Generic spent fuel pool

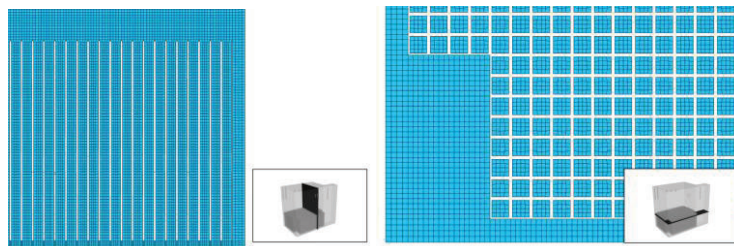


Figure 3 Computational grids (vertical and horizontal cross sections)

The grid (Figure 3) is fully hexahedral and structured. The total amount of cells is about 6 million. Except in the fuel assemblies, friction does not drive the plume flows, hence the non dimensional parameter y^+ (see [3]) does not strictly complies with recommended practices, in order to keep an acceptable number of cells.

3.1.2. CFD code and models

All single phase calculations are performed thanks to the *Code_Saturne* software, release 3.0, developed by the R and D division of EDF [3]. It is a general purpose CFD tool, solving fluid dynamics equations via the *Simplec* algorithm, based on the Patankar's *Simple* procedure [6] and a time marching scheme: A velocity field issued from momentum equation is corrected in order to satisfy the mass balance. This velocity correction comes from a pressure one, obtained via a Poisson equation and using the previous mass balance residual as source term.

Turbulence is modeled, for the present situation, via a RANS (Reynolds Averaged Navier-Stokes) 2nd order model RSM-SSG (Reynolds Stress Model, *Speziale Sarkar Gatski* variant) [3] taking into account the anisotropy of turbulence of the thermal plume.

The liquid is considered as incompressible and the physical properties: density, thermal conductivity, specific heat, molecular viscosity are those of pure water and considered dependent on the temperature. The saturation temperature depends on the pressure. All properties are from reference [11].

3.1.3. Fuel assembly modeling

The geometry scale of the fuel assemblies (rod diameter or grid vanes being centimeter-level or below) favors a homogeneous representation. An equivalent medium with distributed momentum sinks and porosity coefficients models the pressure loss occurring in the fuel assemblies: friction along the rods, singular pressure drops of mixing grids, bottom and top end pieces. Those momentum sinks are given for

the different directions, and depend on the local Reynolds number. Pressure drop and porosity terms have also been added to model the supporting pads of the racks, which are not explicitly represented by the mesh.

Table 1 gives the pressure drop coefficients used for the supporting pads and the fuel assemblies (see also Figure 4):

		Axial (along z axis)	Transverse (along x and y axes)
Supporting pads		0	$1.15 C_x \frac{d}{D(1 - \frac{d}{h})^3}$ Cx=f(Re) : drag coefficient of a cylinder in a transverse flow
Fuel assembly	Re < 2000	$14.2 + \frac{64H}{D_H Re}$	$\frac{64L}{D_H Re}$
	Re > 2000	$14.2 + \frac{0.316H}{D_H Re^{0.25}}$	$2.66 * 17 * Re^{-0.2}$

Table 1 Pressure losses specified

where h is the pad height (0.1 m), H is the assembly height (4.8 m), L the assembly width (0.2 m) and D_H is the hydraulic diameter of the fuel assembly in the axial direction (Re is the Reynolds number).

The momentum sinks are constant along the altitude, i.e. friction and singular pressure drops are summed up and distributed homogeneously along the assembly height. The porosity coefficient α specified in the fluid cells representing the assemblies to get correct vertical velocities matches 0.77. The thermal inertia of solid is hence not taken into account, meaning that decay heat is directly transferred to liquid water only. This penalizing assumption in transient regime has indeed no effect when reaching a steady state.

The rack walls are modeled via two-dimensional plane walls (no thickness). Friction is considered along each face and no heat transfer across them is specified, which is a conservative assumption as regards to a potential thermal homogenization.

The decay heat is prescribed as a volumetric source of the energy equation, this value depends directly on the fuel history and here an average representative value of 20 MW is retained. A generic configuration is retained, i.e. about a quarter of the pool being filled with high power assemblies coming from the reactor core, the rest of the pool being filled with low power fuel assemblies, issued from previous refueling cycles.

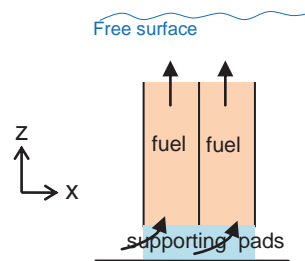


Figure 4 Rack modeling

3.1.4. Initial and boundary conditions

Table 2 provides the dynamic and thermal boundary conditions for both the initial phase and the pump restart transient.

The initial conditions of the steady state calculations are uniform: $V_x=V_y=V_z=0$ and $T = 97^\circ\text{C}$.

The initial conditions of the transient calculation are the dynamic and thermal fields obtained for the steady state.

	<i>Initial steady state</i>	<i>Restart transient</i>
<i>Pool lateral walls</i>	Friction	
	Adiabatic	
<i>Pool bottom wall</i>	Slip wall (pressure loss specified in fluid)	
	Adiabatic	
<i>Free surface (top boundary)</i>	Slip wall	
	Heat transfer with atmosphere at $T_a=50^\circ\text{C}$: $Nu=0.14Ra^{1/3}$ [12]	
<i>Water inlet</i>	Friction	$V_x=V_y=0$ $V_z=-1,7$ m/s
	Adiabatic	$T = 25^\circ\text{C}$
<i>Water outlet</i>	Friction	$V_x=V_y=0$ $V_z=0.8$ m/s
	Adiabatic	(Outward flow)

Table 2 Boundary conditions

(Nu and Ra are the Nusselt and Rayleigh numbers, V_i is the velocity in the i direction)

3.1.5. Boiling approximation

The boiling model set in the single phase formulation is defined as:

- The vapor produced does not modify the flow itself: it is supposed to occur close to the free surface so that bubbles can easily be transferred into the surrounding atmosphere with a low momentum transfer to water.
- The temperature of the pool does not exceed the saturation value (which depends on the altitude and more precisely on the local static pressure): a sink term is prescribed, it corresponds to the liquid evaporated. This technique supposes that once evaporated, the steam cannot condense elsewhere in the pool. This hypothesis, a priori, restrictive, is in fact well verified since bubbles (vaporization) occur during a rising flow to the surface, with a saturation pressure decreasing at the same time.

The heat sink is therefore simply represented by limiting the temperature (T_c) to the saturation one (T_{sat}): for each computational cell, if ($T_c > T_{sat}$) at the end of the time step, T_c is set to T_{sat} . The corresponding heat sink can be computed as $S = \sum_{cells\ i} \rho_i v_i Cp(T_{ci} - T_{sat})$ and the evaporated mass

as $M_e = \frac{S}{L_v}$ (v , ρ and Cp being the cell volume, density and specific heat). The heat sink can

also be checked by energy balances at steady states.

3.2. Validation with In-situ Measurements

In order to consolidate the method, the present model is first applied on a true nuclear power plant case and compared to available in-situ measurements. Three vertical temperature profiles (*prf1*, *prf2* and *prf3*) have been recorded during both:

- a steady normal operation,
- a 2-hours transient situation with the forced cooling circuit stopped. This test has obviously been stopped before boiling occurs but the reorganization of the flow patterns can be observed and brings relevant elements for the validation.

The computational domain has been adapted to the actual pool geometry. Pressure drops of the rack cells are modified to fit the design of this pool. Moreover, the power distribution inside each fuel assembly has been assessed from its actual history and is given as an input map of heat source. The pool walls are considered as adiabatic.

The different assemblies appear on Figure 5 (right hand side), each color corresponding to a power level. Measurement profiles are also provided in a normalized format on this figure (left hand side graphs).

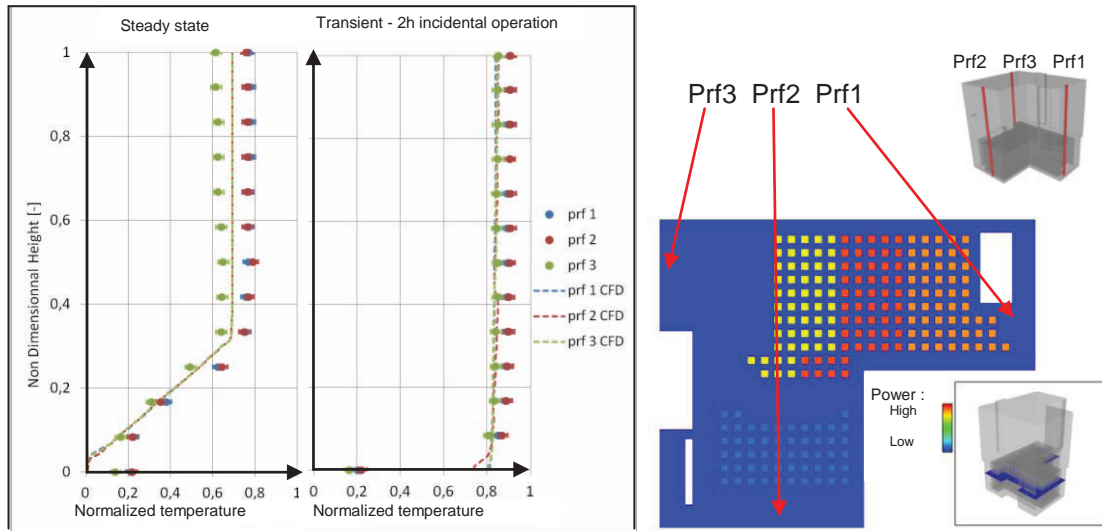


Figure 5 Vertical temperature profiles - Model validation -Top view of pool used for validation, location of temperature measurements

For the steady state (left hand side plot), the general behavior, as a gradient corresponding to the assemblies and the mixed region upon, is found. The vertical gradient and the level of temperature in the homogenous region are well calculated. The validation is in fact relative to the general behavior of the flow inside the pool, since the equilibrium temperature reached in the upper part of the pool is driven by the fuel decay power and the cooling flow rate.

Nevertheless, the slight spatial dissymmetry seen between the 3 thermocouple rakes is not predicted. Authors consider it may be due to wall heat losses in the real pool, not taken into account in calculations with adiabatic boundary conditions.

For the situation 2 h after cooling circuit stop, the homogeneity is obtained and if we consider rakes 1 and 2, the temperature rise is accurately predicted.

3.3. Application

The model is applied to the generic pool configuration, with no cooling flow rate. The calculation is run in a time marching mode towards the asymptotic steady solution, during about 3 h of physical calculation. The recording of different probes (Figure 6) located in computational domain shows that an asymptotic mode is obtained after about 1 hour. In this state, the power released by the spent fuel is equal to the latent heat of the vaporized water in the boiling region.

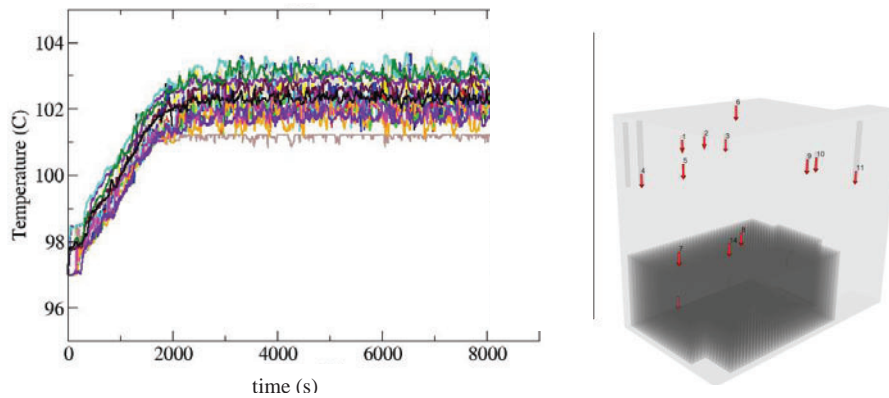


Figure 6 Temperature at probes vs. time (left) and location of probes (right)

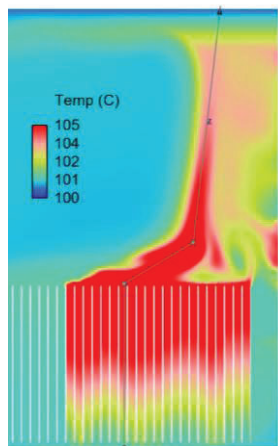


Figure 7 Vertical cross section of temperature at asymptotic state

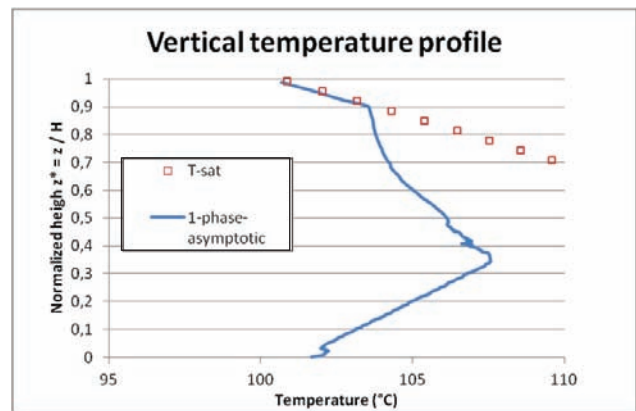


Figure 8 Vertical temperature profile at asymptotic state

Figure 7 presents a vertical cross section of the temperature field, the most powerful fuel assemblies (recent unloaded fuel) produce a hot plume. The later is deviated due to a large natural convection recirculation over the racks.

A vertical plot (along a piecewise straight line shown in Figure 7) is given in Figure 8. Temperature increases as water flows upwards in the fuel, and then decreases thanks to the mixing with the bulk water over the racks. The heat sink is here (since wall exchanges are neglected) the vaporization of water when boiling occurs. The later is located in the upper part of the pool where pressure is decreasing (flashing phenomenon). It is linked to the decrease of the local static pressure. In the pool configuration the static pressure is mainly due to the hydrostatic component (low velocities) so that the local saturation temperature approximately depends only on elevation (depth below the free surface) and considering the room atmospheric pressure in the pool building.

The saturation temperature defined thereby is plotted on Figure 8 (as red hollow squares) and the temperature vertical profile matches this curve from about 1/10th of the pool water height.

Multiple isosurfaces of temperature are plotted on Figure 9, this 3D view explains more precisely the plume effect, the heat removal close to the surface and the mixing due to cold layers driven downwards in the lateral walls region.

Figure 10 provides more details on the zone where boiling occurs when stabilization is reached. This area is mainly the result of the hydrostatic effect which appears as the governing phenomenon. Secondly, it is deformed by the plume effect. This plume effect leads to a rather small dissymetry in the area upon the racks.

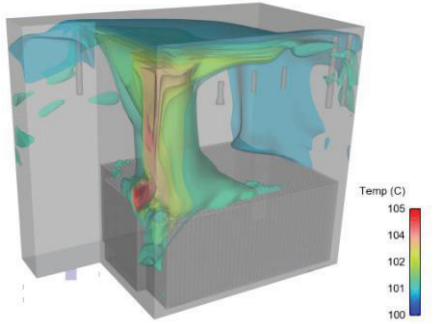


Figure 9 isosurfaces of temperature

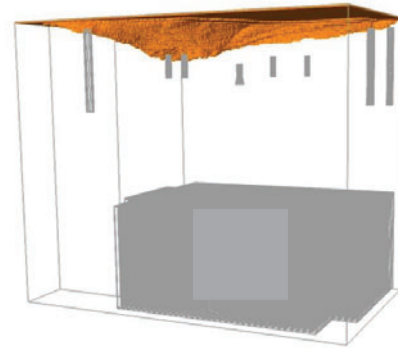


Figure 10 Boiling region

The next section analyzes the restart of the forced cooling circuit. Only one cold water injection is considered (degraded mode, see Figure 2). Temperature iso-surfaces vs. time presented on Figure 11 show that the flow behavior at cooling circuit restart evolves from a natural circulation plume over hottest assemblies to a stratified flow driven by cold water injection. During the transition from natural circulation to stratified distribution of temperature, the hot water plume is disturbed and may transitorily reach the cooling system intakes.

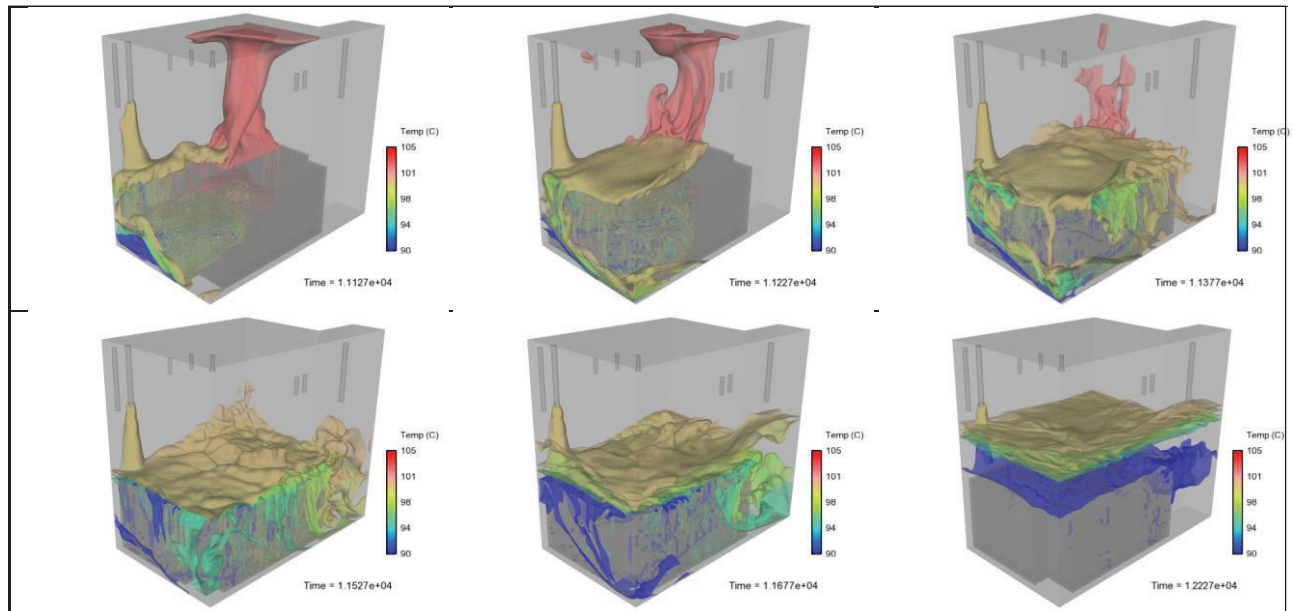


Figure 11 Isosurfaces of temperature - Restart

The potential issue during the restart phase would be to reach saturation temperature inside the cooling circuit and its pumps. Figure 12 gives the temperature obtained at the different water intakes at steady state and after restarting cooling pumps, highlighted at time = 10000 s. A temporary increase of the temperature at two of the intakes occurs, due to hot water plume disturbance. A further CFD calculation of the cooling circuit itself using pool calculations results as inlet conditions allows assessing the risk of cavitation. Literature correlations ([8] for example) are also useful.

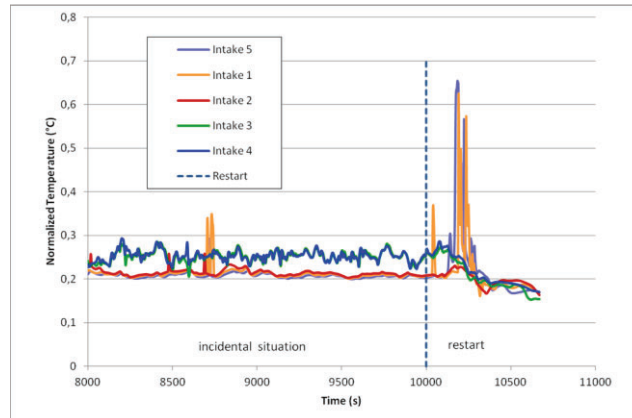


Figure 12 Temperature at intakes – Restart

4. TWO-PHASE MODEL

4.1. Modeling

4.1.1. Domain and grid

The two-phase modeling is based on the same geometrical domain and grid as the single-phase one. The domain is extended upwards along 2 m, to represent the air surrounding the pool surface and to allow the representation of the free surface.

4.1.2. CFD code

The multiphase Neptune_CFD code ([4], [5]), developed within the joint R&D project *Neptune* (EDF / CEA / Areva-NP / IRSN), is used. It solves different phases in an Eulerian approach with the assumption of a common pressure for all fields, following the classical model of Ishii [9]. Three balance equations per field solve the mass, momentum and energy balances. The turbulence is taken into account via the second order Reynolds-Stress Model SSG for the liquid phase.

In order to represent physically the phenomena in the present configuration, three fields (two continuous, one dispersed) are in fact considered:

- (Continuous) liquid water (phase 1)
- (Dispersed) steam bubbles (phase 2)
- (Continuous) atmosphere made of air and steam (phase 3)

This is necessitated to model at the same time both the boiling (flashing) phenomenon and the free surface, the latter interacts therefore with a third phase which is not directly the vapor bubbles.

The following interactions are taken into account:

- Steam bubbles / liquid water: The momentum transfer is simulated via the drag force of Ishii [7] and an in-house turbulent dispersion model (“GTD”, for Generalized Turbulent Dispersion, see Laviéville et al. [13]).

- (Continuous) air / liquid-water interface: This represents the free surface.
- Air - steam: The steam bubbles rising at the surface become a component of the atmosphere.

4.1.3. Initial and boundary conditions

The boundary conditions are similar to those specified for the single phase, steady state computation. However, the pool free surface is now a part of the domain and the top boundary is a wall. The boundary conditions are therefore:

- *Lateral walls*: friction for both phases, adiabatic,
- *Bottom wall*: slip wall for both phases, adiabatic,
- *Top wall*: friction for both phases, adiabatic.

The initial conditions are:

- temperature = 97°C,
- zero velocity,
- pool itself : 100% liquid water,
- upper atmosphere : 100% gas : components : air 100%, steam 0% (simplification, there is not impact of the initial moisture on the pool boiling behavior).

4.1.4. Free surface model

The interfacial exchanges at the free surface are modeled with an in-house set of dedicated methods known as the “Large Interface Model” (LIM), mainly developed by Coste [10]) suited to represent interfaces larger than the cell size, and initially developed for the Pressurized-Thermal Shock (PTS) application. It includes large interface recognition, interfacial transfer of momentum, potential heat and mass transfer with direct contact condensation. The LIM can simulate large interfaces which can be smooth, wavy or rough, its implementation involves a three-cell stencil: one for the liquid phase, one for the gas phase and one for the intermediate region.

4.1.5. Boiling model

The energy transfer between liquid and steam bubbles is driven via a flashing model ensuring the return to saturation of liquid particles, derived from the model implemented in the *Cathare* system code [14]. The heat transfer from water to steam $Q_{w/s}$ is calculated as $Q_{s/w} = -c(h_1 - h_1^{sat})$, h_1 being the liquid enthalpy and c a coefficient taking into account a delay for the return to saturation (see [14] for details).

4.1.6. Surrounding atmosphere

The gas layer upon the pool itself is made of air initially. During the event, a source term of steam (corresponding to the bubble phase rising to the surface) is specified, it is treated as a scalar via a transport diffusion equation. At the interface the steam mass flux is therefore transferred from the dispersed gas phase 2 to the continuous gas phase 3. This mass transfer is done with no momentum and no heat exchange.

4.2. Application

The initial objective is to simulate the transient presented in section 3, i.e. the loss of forced cooling circuit followed by one pump restart. Moreover the use of a two-phase formulation allows also modeling explicitly the drop in water level and the periodic water replenishment.

The complexity of the three-phase model associated with long physical times led to heavy computational times. Hence, this paper presents the solution after a rather short time period of 20 min.

Figure 13 shows the vertical temperature profile, compared to the single phase approach and to the saturation temperature based on the hydrostatic pressure. According to Figure 6, the asymptotic state cannot be reached after 20 min. Moreover a real asymptotic state will not be rigorously reached since there are both a water level drop and periodic replenishments.

However, Figure 13 shows an agreement on the thermal behavior between single-phase and two-phase approaches, the shapes of both profiles are quite comparable. So, if we consider that the multi phase model is more precise since it integrates more physics, the conclusion after 20 min of physical transient is that the approximations made in the single-phase approach would lead to a correct prediction (boiling by flashing below the surface, no recondensation). Further calculations must be carried out to draw a conclusion at steady state with maximum boiling.

The temperature cross section (Figure 14) and iso-surfaces (Figure 15) of temperature show the thermal plume generated by the hot fuel assemblies. In addition, it should be noted that the flow appears more instable, especially in the fuel assemblies, than for the single phase approach. This will have to be further investigated at steady state.

Figure 16 represents the free surface (blue surface), which is found almost flat, with few disturbances. The sepia surface is an iso-surface of steam fraction ($C = 0.01$). The part below the free surface can be compared with the boiling region of the single phase approach plotted on Figure 10. A qualitative agreement is found. The part upon the free surface corresponds to the mixing inside the air surrounding the pool.

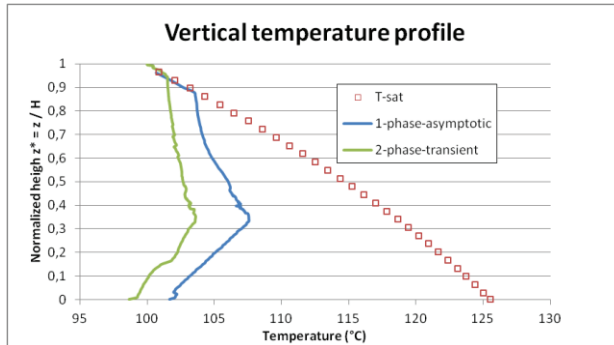


Figure 13 Vertical temperature profiles compared

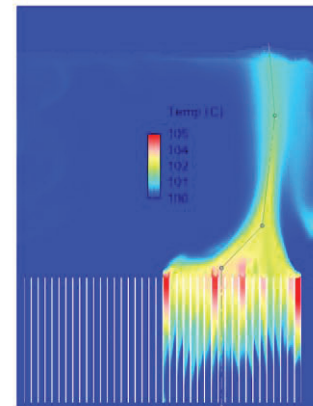


Figure 14 Temperature in a vertical cross section at intakes - Two-phase model

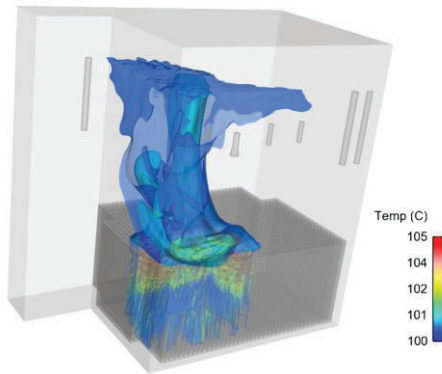


Figure 15 Iso-surfaces of temperature Two-phase model

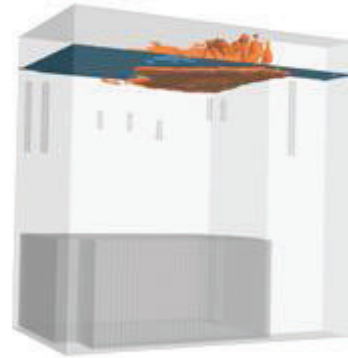


Figure 16 Free surface and steam fraction

5. CONCLUSION

This paper presents both single phase and two phase approaches to model and better understand the thermal and hydraulic behavior of a spent fuel storage pool in conditions of loss of forced cooling circuit with constant liquid water level. Since the objective is the definition of a methodology, a generic pool is considered. The main conclusions are:

- A single phase calculation implies strong hypotheses, but is able to provide first results as the boiling occurrence (in time and in space), the global thermal hydraulic flow and the saturation margins.
- A multiphase modeling requires dealing with the free surface phenomenon and with the boiling itself. This necessitates in the Neptune_CFD code the use of 3 fields and defining subsequent interfacial exchanges.
- The first results show the relevance of the simplifying hypotheses of the single phase model.
- A multi-phase computational brings additional informations such as representation of the free-surface exchanges and the atmosphere behavior

The next steps will be to:

- Terminate the present multiphase computation in order to make a full comparison with the single phase one and to state on the advantages of this more sophisticated model at steady state with full pool boiling.
- Compare with experimental results on a further test case and improve the implementation.

The application to industrial cases for design or safety demonstration will be envisaged later on a further step, when the methodology is defined precisely and validated.

ACKNOWLEDGMENTS

The authors are grateful to Mathieu Guingo and Cyril Baudry from Électricité de France for their help on Neptune_CFD code.

REFERENCES

1. Hung, T.-C., Dhir, V. K., Pei, B.-S., Chen, Y.-S., Tsai, F. P., “The development of a three-dimensional transient CFD model for predicting cooling ability of spent fuel pools”, *Applied Thermal Engineering*, **50**,

- 2013, pp. 496-504.
2. Boyd, C. F. "Predictions of Spent Fuel Heat up After a Complete Loss of Spent Fuel Pool Coolant", NUREG-1726, U.S. Nuclear Regulatory Commission, June 2000.
 3. Archambeau, F., Mechtoua, N., Sakiz, M., "Code_Saturne: a Finite Volume Code for the Computation of Turbulent Incompressible Flows - Industrial Applications," *International Journal on Finite Volumes*, vol. 1, 2004.
 4. Douce, A., Mimouni, S., Guingo, M., Morel, C., Laviéville, J., Baudry, C., "Validation of Neptune_CFD 1.0.8 for adiabatic bubbly flow and boiling flow", *proceedings of the CFD4NRS-3 conference*, Washington DC, USA, 2010.
 5. Mimouni, S., Baudry, C., Denèfle, R., Fleau, S., Guingo, M., Hassanaly, M., Laviéville, J., Méchtoua, N., Méricoux, N., "Multifield Approach and Interface Locating Method for Two-Phase Flows in Nuclear Power Plant", *proceedings of the CFD4NRS-5 conference*, September 9-11 2014, Zurich, Switzerland.
 6. S.V. Patankar, "Numerical heat transfer and fluid flow", Series in computational methods in mechanics and thermal sciences, McGraw-Hill book company, New-York, 1980, 197 p.
 7. M. Ishii and N. Zuber, "Drag coefficient and relative velocity in bubbly, droplet or particulate flows," *AIChE Journal*, vol. 25.
 8. Tullis, J. P., "Modeling Cavitation for closed conduit flow", *J. Hydraul. Div. ASCE*, **107**(HY11), Proc. Paper 16650, November 1981, pp. 1335-1349.
 9. Ishii, M., "Thermo-fluid dynamic, theory of two-phase", Collection de la Direction des Etudes et Recherches d'Electricité de France, n°22, Eyrolles, Paris, 1975, 275 p.
 10. Coste, P., "A large interface model for two-phase CFD", *Nuclear Engineering and Design*, vol. **255**, Feb. 2013, pp. 38-50. (<http://dx.doi.org/10.1016/j.nucengdes.2012.10.008> (2012)).
 11. W. Wagner et al., "The IAPWS Industrial Formulation 1997 for the Thermodynamic Properties of Water and Steam," *ASME J. Eng. Gas Turbines and Power*, 122, 150-182 (2000).
 12. W.H. McAdams, "Heat transmission", 3rd edition, McGraw-Hill publishing company ltd, London, 1954, 532p.
 13. Laviéville, J., Méricoux, N., Guingo, M., Baudry, C., Mimouni, S. "A Generalized Turbulent Dispersion model for bubbly flow numerical simulation in NEPTUNE_CFD", *Proceedings of NURETH-16*, Chicago, IL, USA, Sept. 2015.
 14. Serre G., Bestion D.: Physical Laws of CATHARE Revision 6. Pipe Module. CEA report SMTH/LMDS/EM/98-038, September 1999.